Inorganic Chemistry

Article

pubs.acs.org/IC

Synthesis and Structural Characterization of High Spin M/Cu (M = Mn, Fe) Heterobimetallic and Fe/Cu_2 Trimetallic Phosphinoamides

Subramaniam Kuppuswamy,[†] Benjamin G. Cooper,[†] Mark W. Bezpalko,[†] Bruce M. Foxman,[†] Tamara M. Powers,[‡] and Christine M. Thomas*[,†]

[†]Department of Chemistry, Brandeis University, 415 South Street, Waltham, Massachusetts 02454, United States

[‡]Department of Chemistry and Chemical Biology, Harvard University, Cambridge, Massachusetts 02139, United States

Supporting Information

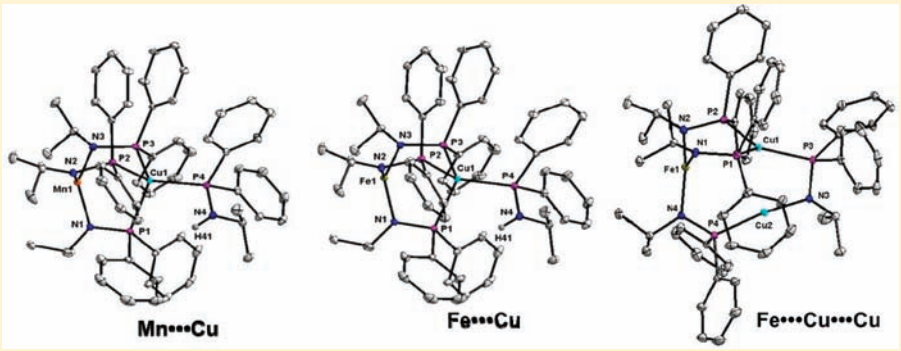

ABSTRACT: The heterobimetallic complexes $[Mn(^{i}PrNPPh_2)_3Cu(^{i}PrNHPPh_2)]$ (**1**) and $[Fe(^{i}PrNPPh_2)_3Cu(^{i}PrNHPPh_2)]$ (**2**) have been synthesized by the one pot reaction of $LiN^{i}PrPPh_2$, MCl_2 (M = Mn, Fe), and CuI in high yield. Addition of excess CuI into **2** or directly to the reaction mixture led to the formation of a heterotrimetallic $[Fe(^{i}PrNPPh_2)_3Cu_2(^{i}PrNPPh_2)]$ (**3**) in good yield. Complexes **1**−**3** have been characterized by means of elemental analysis, paramagnetic ^{1}H NMR, UV−vis spectroscopy, cyclic voltammetry, and single crystal X-ray analysis. In all three complexes, Mn or Fe are in the +2 oxidation state and have a high spin electron configuration, as evidenced by solution Evans' method. In addition, the oxidation state of Fe in complex **3** is confirmed by zero-field ^{57}Fe Mössbauer spectroscopy. X-ray crystallography reveals that the three coordinate Mn/Fe centers in the zwitterionic complexes **1**−**3** adopt an unusual trigonal planar geometry.

INTRODUCTION

Studies of heterobimetallic complexes have become an important area of research inspired by the effects of metal−metal cooperativity on structural, electronic, and multielectron redox properties.[1−4] In addition to their potential roles in catalytic processes, bimetallic combinations, particularly those featuring two late transition metals, are found in the active sites of many metalloenzymes, including carbon monoxide dehydrogenases,[5,6] acetyl-coenzymeA synthase,[5,6] heme-copper oxidases,[7] and hydrogenases.[8,9] The design of new heterobimetallic complexes presents a challenge in comparison to monometallic or homobimetallic complexes, as linking two electronically different metal centers in close proximity to each other is highly dependent on ligand architecture and close matching of the hard/soft donor/acceptor properties of the metal and ligand. To overcome these difficulties, our group has built upon the early work of Nagashima and co-workers[10−13] and utilized phosphinoamide ligand frameworks to explore the chemistry of early/late heterobimetallic complexes featuring a Group IV metal linked to a Co center (Chart 1).[14−17] Using this design, our group has recently uncovered enhanced Co redox properties,[14] unique reduced complexes featuring Co−Zr multiple bonds,[15] and a number of small molecule activation processes.[16,18,19]

We now turn our attention to bimetallic complexes featuring two late transition metals in disparate coordination environments. While a large number of late/late heterobimetallic complexes have been reported, these are typically formed using bridging ligands that present similar (hard/hard or soft/soft) donors to each metal and, thus, lead to metals in similar electronic environments.[20,21] An interesting new class of bimetallic species, termed "xenophilic" complexes, are composed of metal−metal interactions between one hard open-shell metal and a second soft metal typically supported by carbonyls.[22] Theoretical investigations have suggested that the two vastly different coordination environments on the two late transition metals in xenophilic complexes lead to unusual electronic properties and magnetic behavior.[23] Moreover, Lindahl has recently posed the theory that disparities in metal electronic properties and the resultant metal−metal

Received: October 6, 2011
Published: January 18, 2012

   dx.doi.org/10.1021/ic202165z | *Inorg. Chem.* 2012, 51, 1866−1873

Chart 1

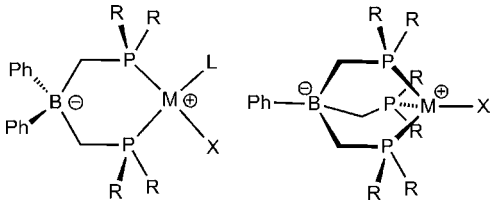

Peters et al.[26-36]

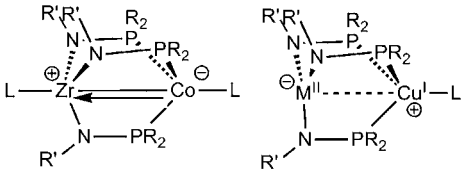

Thomas et al.[14-19] This work

interactions are responsible for the functionality of bimetallic enzyme active sites in catalysis.[24]

Both early/late and late/late heterobimetallic complexes are particularly interesting in light of the potential for the formation of formally zwitterionic complexes featuring charge separation between a cationic metal fragment and an anionic metal fragment. Zwitterionic complexes composed of negatively charged ancillary ligands, most prominently borates, and positively charged late metal fragments have received considerable attention in the recent literature.[25] In terms of zwitterionic complexes featuring phosphine ligands, the most well-studied are the late metal bis- and tris(phosphino)borate ligands of Peters and co-workers (Chart 1).[26−36] While many of the advantages of tethering the counterion to the ligand are derived from solubility and tolerance to polar solvents, there is also convincing evidence that the close proximity of the negatively charged borate affects the electron density at the metal center.[26,27,29,30,34] In this light, it is interesting to consider the aforementioned heterobimetallic Zr/Co complexes reported in our own work.[14,15,17] As shown in Chart 1, the doubly reduced Zr/Co complexes are formally zwitterionic, with a positive formal charge residing on the Zr^{IV} center and a negative formal charge on the Co^{-I} atom. In this case, the proximity of the two ions has a clear effect on both redox potentials and reactivity at the metal centers and dative bond formation between the charged atoms is inevitably observed.[14−19] Herein we report the synthesis and characterization of heterometallic (Mn/Cu and Fe/Cu) phosphinoamides, and investigate the effect of the zwitterionic nature of these species on the electronic environment of the two metal centers.

RESULTS AND DISCUSSION

Synthesis and Characterization. Salt metathesis of LiN^iPrPPh_2 (generated in situ) with a 1:1 mixture of $MnCl_2$ and CuI in one pot affords $[Mn(^iPrNPPh_2)_3Cu(^iPrNHPPh_2)]$ (**1**) as a yellow crystalline solid in 85% yield. Under identical reaction conditions using $FeCl_2$ in place of $MnCl_2$, $[Fe(^iPrNPPh_2)_3Cu(^iPrNHPPh_2)]$ (**2**) is produced as an olive green crystalline solid nearly quantitatively. However, continuous stirring (more than 24 h) of the reaction mixture used to generate **2** affords an orange crystalline solid, $[Fe(^iPrNPPh_2)_3Cu_2(^iPrNPPh_2)]$ (**3**), along with unidentified insoluble byproducts. Complex **3** can also be prepared independently by an alternative route via addition of excess CuI to **2** or by one pot synthesis with excess CuI. Thus, complex **2** is an apparent isolable intermediate to form **3** and would be a potential precursor to make trimetallic complexes with three different metal ions. Complexes **1**−**3** are air and moisture sensitive, but stable at room temperature for weeks without any decomposition. Notably, complexes **1** and **2** can, alternatively, be synthesized in a stepwise fashion starting with the cationic tris(phosphinoamine) Cu complex $[Cu(PPh_2NH^iPr)_3][PF_6]$ (Scheme 1). Deprotonation of the Cu-

Scheme 1

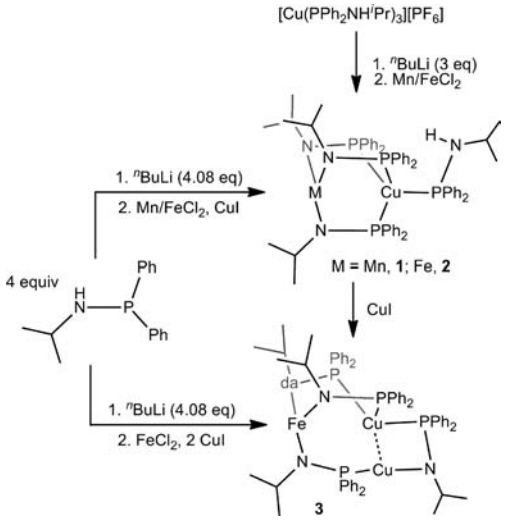

bound phosphinoamines, followed by treatment with $MnCl_2$ or $FeCl_2$, leads exclusively to formation of **1** and **2**, respectively.

The ^1H NMR spectra for **1**−**3** are broad and exhibit large paramagnetic shifts, with chemical shifts between +30 and −32 ppm. The 11 resonances observed for each of these compounds is consistent with a C_3-symmetric bimetallic phosphinoamide core and an inequivalent terminal phosphinoamine ligand. Interestingly, 10 broad resonances are observed between +26 and −13 ppm in the ^1H NMR spectrum of **3**, indicative of only two sets of inequivalent ligand environments at room temperature. The presence of just one set of 5 resonances for the three phosphinoamide ligands bridging Fe and Cu is indicative of fluxional behavior in solution at ambient temperature. We hypothesize that this fluxionality is attributed to the rapid intramolecular exchange of the phosphine donors of the bridging phosphinoamides via ligand exchange between the Cu centers. Solution Evans' method measurements are indicative of $S = 5/2$ ($\mu_{eff} = 5.77\ \mu_B$) and $S = 2$ ($\mu_{eff} = 4.90$ and $4.89\ \mu_B$) ground states for **1**, **2**, and **3**, respectively, consistent with high spin Mn(II) and Fe(II). The protonated state of the terminal phosphinoamine ligand in **1** and **2** is evidenced by characteristic infrared N−H stretching frequencies at 3389 and 3366 cm^{-1}, which are comparable with the ν(N−H) of free phosphinoamine ligand (3360 cm^{-1}). While the origin of the nitrogen-bound proton remains unknown, it is worth noting that isolating the LiN^iPrPPh_2 salt prior to reaction with the two metal salts leads to **1** and **2** exclusively, indicating that the protonated ligand bound to Cu in these complexes does not result from incomplete deprotonation.

dx.doi.org/10.1021/ic202165z | Inorg. Chem. 2012, 51, 1866−1873

The oxidation state of **3** is further confirmed by zero-field ^{57}Fe Mössbauer spectroscopy, in which a quadrupole doublet centered at δ = 0.65 $^{mm}/_{s}$ (ΔE_Q = 2.05 $^{mm}/_{s}$) is observed (Figure 1). The isomer shift and quadrupole splitting

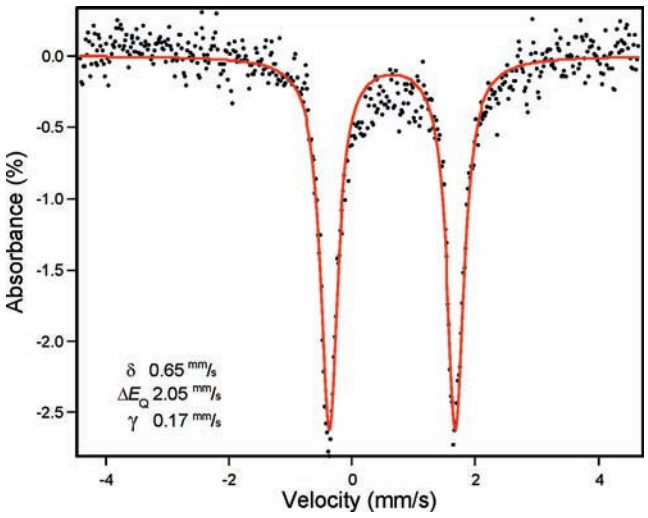

Figure 1. Solid state Mössbauer spectrum of **3** at 110 K.

fall in the range expected for high spin Fe(II),[37] and the isomer shift compares well with that of three-coordinate high spin Fe(II) complexes reported in the literature (~0.6 mm/s to ~0.8 mm/s).[38−42]

X-ray Crystallography. X-ray quality single crystals of **1**−**3** were grown by slow evaporation of concentrated ether solution at room temperature, and the molecular structures are shown in Figure 2. Complexes **1** and **2** are isostructural and composed of three bridging phosphinoamides, in which the hard amide donors are bound to Mn/Fe, while the soft bridging phosphine ligands are ligated to Cu. Complexes **1** and **2** adopt an unusual structure in which the bimetallic core consists of three six-membered $M_2N_2P_2$ rings with a trigonal planar coordination environment at Mn and Fe, respectively ($\Sigma_{N\text{-}M\text{-}N}$ 351.75° for **1**; $\Sigma_{N\text{-}M\text{-}N}$ 356.99° for **2**). The geometries about Mn and Fe in **1** and **2** are largely similar (Table 1); however, the Mn−N distances are slightly elongated with respect to the Fe−N distances as a result of the decreased ligand field stabilization energy for high spin d^5 Mn(II). The distorted tetrahedral coordination sphere of Cu is completed by a terminal phosphinoamine ligand. Interestingly, the divalent metals (Mn/Fe) bind three negatively charged amides while the monovalent Cu centers bind four neutral ligands, resulting in unusual zwitterionic complexes. Interestingly, the avg Cu−P distances associated with the bridging phosphinoamides (2.3747 (5) Å (**1**) and 2.3347 (4) Å (**2**)) are significantly longer than the terminal phosphinoamine Cu−P distance (2.2992(5) Å (**1**) and 2.2984(4) Å (**2**)). For comparison, the monometallic Cu^I complex $ICu(PPh_2NH^iPr)_3]$ (**4**) was synthesized and structurally characterized (see Supporting Information). The average Cu−P distance in **4** (2.255 Å) is significantly shorter than the Cu−P distances associated with the bridging ligands in **1** and **2**, suggesting that metal coordination of the amide moiety withdraws electron-density from the phosphine via resonance.

A single crystal X-ray diffraction study of **3** reveals an asymmetric trimetallic molecule composed of three metal ions bridged by four phosphinoamide ligands. Unlike complex **2**, in **3** the fourth phosphinoamine ligand is deprotonated and bridges to a second copper atom. The three-coordinate Fe1 and Cu1 centers adopt a nearly trigonal planar geometry (Σ_{N-Fe-N} 359.83°; Σ_{P-Cu-P} 359.26°), whereas the geometry about the two-coordinate Cu2 deviates ~10° from linearity. The two-coordinate Cu2−P4 distance (2.1578 (4) Å) is substantially shorter than the other three Cu−P distances that span a range from 2.2584 (4) to 2.2738 (4) Å.

The distance between the metal ions in **1** and **2** are significantly longer than the sum of the covalent radii (2.8734(5) Å (**1**) and 2.9006(3) Å (**2**) vs 2.35 Å, respectively).[43] The three intermetallic distances in the trimetallic core of **3** are Fe1···Cu1 = 2.9691(3) Å, Fe1···Cu2 = 3.734(4) Å, and Cu1···Cu2 = 2.7196(3) Å. The Cu···Cu distance in **3** is in the range of d^{10}-d^{10} interactions reported in the literature.[44] The Fe···Cu distances in **2** and **3** clearly indicate the absence of a bond between Fe and Cu and are substantially longer than those reported in other Fe/Cu bimetallics in the literature as follows: $[Fe(CO)_3(SiOMe_3)(\mu$-

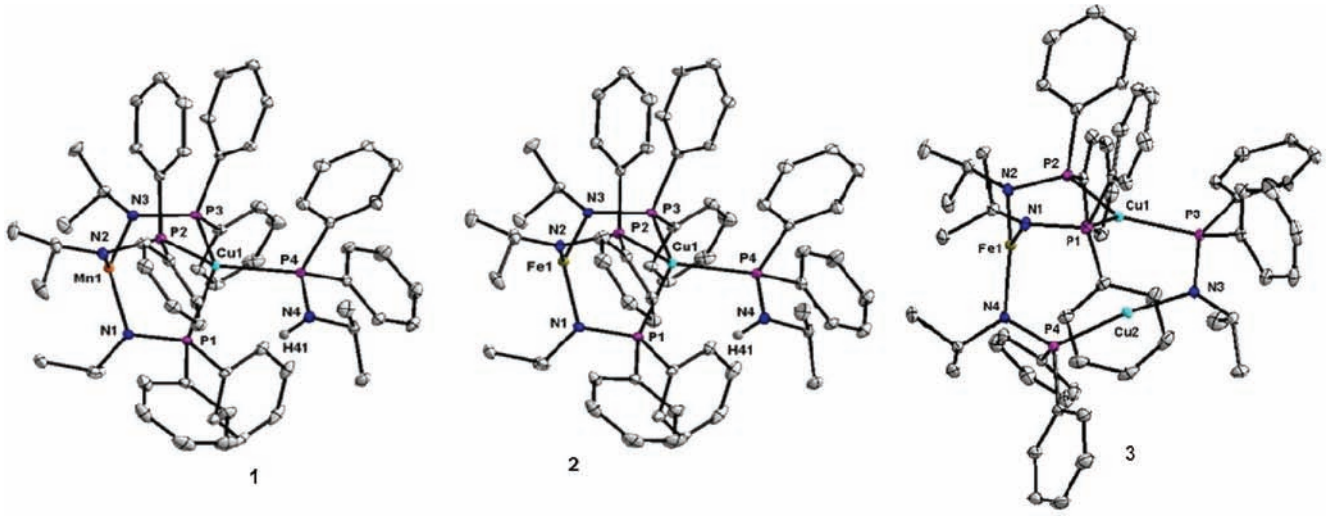

Figure 2. Displacement ellipsoid (30%) representations of **1**−**3**. Hydrogen atoms, except for those bound to phosphinoamine nitrogen atoms, and solvent molecules have been omitted for clarity.

dx.doi.org/10.1021/ic202165z | Inorg. Chem. 2012, 51, 1866−1873

Table 1. Selected Bond Lengths (Å) and Angles (deg) for 1−3

1		2		3	
		Bond Lengths			
Mn1−N1	2.0215(14)	Fe1−N1	1.9653(13)	Fe1−N1	1.9830(13)
Mn1−N2	2.0203(14)	Fe1−N2	1.9652(13)	Fe1−N2	1.9759(13)
Mn1−N3	2.0286(14)	Fe1−N3	1.9701(13)	Fe1−N4	1.9989(13)
Cu1−P1	2.3609(5)	Cu1−P1	2.3551(4)	Cu1−P1	2.2738(4)
Cu1−P2	2.3931(5)	Cu1−P2	2.3867(4)	Cu1−P2	2.2584(4)
Cu1−P3	2.3701(5)	Cu1−P3	2.3621(4)	Cu1−P3	2.2621(4)
Cu1−P4	2.2992(5)	Cu1−P4	2.2984(4)	Cu2−P4	2.1578(4)
Mn1−Cu1	2.8734(5)	Fe1−Cu1	2.9006(3)	Fe1−Cu1	2.9691(3)
				Cu2−N3	1.8626(13)
				Fe1−Cu2	3.734(4)
				Cu1−Cu2	2.7196(3)
		Bond Angles			
N1−Mn1−N2	114.89(6)	N1−Fe1−N2	115.20(6)	N1−Fe1−N2	115.95(5)
N1−Mn1−N3	119.42(6)	N1−Fe1−N3	119.29(6)	N1−Fe1−N4	121.40(5)
N2−Mn1−N3	117.44(6)	N2−Fe1−N3	117.29(6)	N2−Fe1−N4	122.48(6)
P1−Cu1−P2	107.25(2)	P1−Cu1−P2	106.30(2)	P1−Cu1−P2	114.86(2)
P1−Cu1−P3	107.06(2)	P1−Cu1−P3	106.49(2)	P1−Cu1−P3	120.81(2)
P1−Cu1−P4	107.14(2)	P1−Cu1−P4	107.68(2)	P2−Cu1−P3	123.59(2)
P2−Cu1−P3	102.71(2)	P2−Cu1−P3	101.51(2)	P3−Cu2−P4	156.72(2)
P2−Cu1−P4	114.42(2)	P2−Cu1−P4	115.34(2)	P4−Cu2−N3	170.33(4)
P3−Cu1−P4	117.66(2)	P3−Cu1−P4	118.61(2)	N3−Cu2−N4	163.33(4)

Table 2. Redox Potentials of 1−4, Ph_2PNH^iPr, and $[^iPrNLiPPh_2(THF)]_2$, Determined Using CV[a]

	ligand-based oxidation	$M^{III/II}$ (M = Fe or Mn)	$Cu^{I/0}$
Ph_2PNH^iPr	0.57 V, 0.83 V		
$[^iPrNLiPPh_2(THF)]_2$	0.51 V		
$[ICu(PPh_2NH^iPr)_3]$ (**4**)	0.40 V, 0.79 V		−2.99 V
$[Mn(^iPrNPPh_2)_3Cu(^iPrNHPPh_2)]$ (**1**)	0.50 V, 0.70 V	0.40 V	
$[Fe(^iPrNPPh_2)_3Cu(^iPrNHPPh_2)]$ (**2**)	0.48 V, 0.90 V	−0.60 V	
$[Fe(^iPrNPPh_2)_3Cu_2(^iPrNPPh_2)]$ (**3**)	0.90 V	−0.33 V	−2.77 V

[a] In 0.40 M $[^nBu_4N][PF_6]$ in THF.

$Ph_2PCH_2PPh_2)Cu(PPh_3)]$ = 2.540(2) Å,[45] $[Fe(CO)_3(POMe(NMe_2)_2)(\mu\text{-}Si(OMe)_2NMe_2)Cu(PPh_3)]$ = 2.530(2) Å,[46] $[Fe(CO)_3(\mu\text{-}PPh_2Py)Cu(Me_2CO)]^+$ = 2.501(2) Å,[47] $[Fe(CO)(CO)_2(\mu\text{-}Ph_2PCH_2N(Morpholine))Cu]^+$ = 2.550(1) Å,[48] $[Fe(CO)_3(\mu\text{-}Ph_2PCH_2NPy(C_6H_{11}))Cu]^+$ = 2.4572(7) Å,[49] and $[Fe(CO)(CO)_2(\mu\text{-}Ph_2PCH_2N(Oxazoline))Cu]^+$ = 2.5441(7) Å.[50] Likewise, the Mn···Cu in **1** is much longer than previously reported Mn/Cu complexes, including (bis(o-dimethylarsinophenyl)methylarsine)$CuMn(CO)_5$ (2.56(1) Å),[51] (en)$Cu(\mu\text{-}CO)_2Mn(CO)_3$ (2.44(2) Å, en = ethylenediamine),[52] and (dien)$Cu(\mu\text{-}CO)Mn(CO)_4$ (2.48(1) Å, dien = diethylenediamine).[52]

Cyclic Voltammetry. The redox properties of **1**−**3** were investigated using cyclic voltammetry (CV) and reveal exclusively irreversible redox processes for bimetallic complexes **1** and **2** (see Supporting Information), while **3** appears to undergo an quasi-reversible reduction. Since redox events centered at the phosphinoamide ligand, the late metal (Fe or Mn), and Cu are all possible, the CV of the phosphinoamine ligand Ph_2PNH^iPr, the isolated lithium amide $[^iPrNLiPPh_2(THF)]_2$, and the monometallic tris(phosphinoamine) Cu^I complex $ICu(PPh_2NH^iPr)_3$ (**4**) were also recorded. The redox potentials for **1**−**4**, Ph_2PNH^iPr, and $[^iPrNLiPPh_2(THF)]_2$ are listed in Table 2.

Given that the CV of the phosphinoamine Ph_2PNH^iPr displays two irreversible oxidation processes while the CV of deprotonated $[^iPrNLiPPh_2(THF)]_2$ has a single irreversible oxidation, it can be surmised that the phosphine portion of the ligand undergoes an oxidation around 0.5 V, while an amine-based oxidation occurs at more positive potential (0.83 V). Similar phosphine-based oxidations are observed at more positive potentials for complexes **1**−**4**, as coordination to Cu decreases the electron density at phosphorus. The oxidations around 0.5 V observed for complexes **1**−**2** and **4** are assigned as amine-based oxidative events, and a similar oxidative wave is absent from the CV of **3** since all four phosphinoamide ligands are deprotonated in the latter complex.

In light of these ligand-based oxidation assignments, the remaining irreversible oxidations are assigned to Mn and Fe, since it appears from the CV of **4** that Cu^{II} is not accessible with this ligand set. The CV of Mn/Cu complex **1** reveals an irreversible oxidation at 0.40 V vs Fc, while the Fe/Cu complexes **2** and **3** have irreversible oxidations at −0.60 V and −0.33 V, respectively. These oxidative events are assigned as $Mn^{III/II}$ and $Fe^{III/II}$ oxidations. The ease of oxidation of Fe^{II} with respect to Mn^{II} is consistent with the stability of the half-filled d shell of the Mn^{II} center, and the $Fe^{III/II}$ oxidation potentials are in line with the oxidation potential (−0.39 V vs Fc) for the tris(amido)Fe^{II} complex reported by Borovik and co-workers (also irreversible).[53] The increase in $Fe^{III/II}$ oxidation potential upon addition of a second Cu atom can be attributed to the withdrawal of electron density from Fe through resonance as a

dx.doi.org/10.1021/ic202165z | Inorg. Chem. 2012, 51, 1866−1873

result of coordination of one phosphinoamide ligand to a linear two-coordinate Cu^{I} center (supported by computational results, vide infra).

Lastly, the CVs of both the ligand and complexes **1**–**2** did not reveal any well-defined reductive events. In contrast, complex **3** appears to undergo a quasi-reversible reduction at −2.77 V vs Fc (Figure 3, Table 2). Since the monometallic Cu

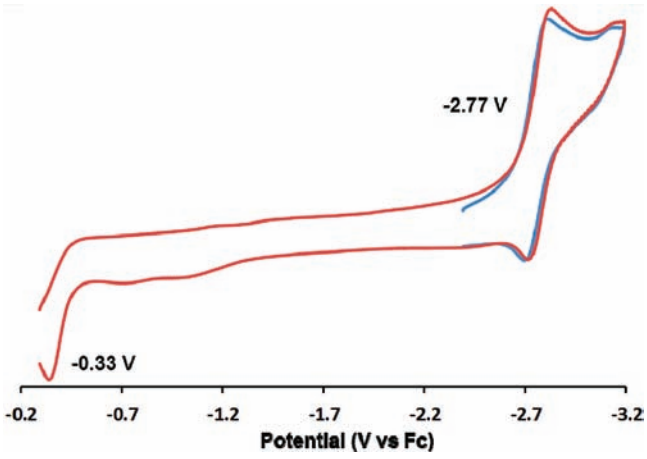

Figure 3. Cyclic voltammogram of complex **3** (2 mM in 0.40 M [$^{n}Bu_4N$][PF_6] in THF, scan rate: 100 mV/s).

complex **4** also undergoes a reduction at −2.99 V (irreversible), these reductive events are assigned as $Cu^{I/0}$ reductions. The Cu centers in **1** and **2** are more electron-rich than that in **3** as a result of an additional phosphine donor ligand (supported by computational results, vide infra), resulting in the absence of $Cu^{I/0}$ reduction outside the accessible solvent window.

Theoretical Investigations. To assess the effects that the close proximity of the two late metal centers in zwitterionic complexes **1**–**3** have on the electronic environment of the individual metal centers, a theoretical investigation was performed using density functional theory (DFT) as implemented by Gaussian 09.[54] A geometry optimization was performed on complexes **2** and **3** starting from coordinates determined via X-ray crystallography. In addition, calculations were performed on the cationic Cu complex [Cu($PPh_2NH^{i}Pr$)$_4$]$^+$ and the anionic Fe complex [Fe($N^{i}PrPPh_2$)$_3$]$^-$ as monometallic comparisons. Subsequent natural population analysis (NBO 3.1) revealed the natural atomic charges listed in Table 3.

Table 3. Natural Atomic Charges Derived from Natural Population Analysis (NBO 3.1) of 2 and 3 and the Monometallic Model Complexes [Cu($PPh_2NH^{i}Pr$)$_4$]$^+$ and [Fe($N^{i}PrPPh_2$)$_3$]$^-$

	Fe	$Cu_{P\text{-bound}}$	$Cu_{P/N\text{-bound}}$
[Fe(^{i}PrNPPh$_2$)$_3$Cu(^{i}PrNHPPh$_2$)] (**2**)	0.933	−0.151	
[Fe(^{i}PrNPPh$_2$)$_3$Cu$_2$(^{i}PrNPPh$_2$)] (**3**)	0.975	0.056	0.473
[Cu($PPh_2NH^{i}Pr$)$_4$]$^+$		−0.117	
[Fe($N^{i}PrPPh_2$)$_3$]$^-$	0.892		

As revealed through a comparison of the natural atomic charge of Fe in complexes **2**, **3**, and [Fe($N^{i}PrPPh_2$)$_3$]$^-$, the electron density at the anionic Fe center in the bimetallic Fe/Cu and trimetallic Fe/Cu_2 complexes is diminished as a result of the pendant Cu^{I} cation. Likewise, the cationic Cu center in bimetallic **2** is more electronic rich than that in [Cu($PPh_2NH^{i}Pr$)$_4$]$^+$ as a result of the appended Fe^{II} anion. Although the bimetallic Mn/Cu complex **1** was not investigated computationally, it is reasonable to assume that similar electronic effects are present in this bimetallic species as well. As predicted based on CV, the charge on both the Fe and Cu centers in **3** are increased by addition of a second Cu atom.

CONCLUSION

In conclusion, we have synthesized and characterized tris(phosphinoamide)-supported heterobimetallic M/Cu (where M = Mn and Fe) complexes. Because of hard/soft ligand preferences, the ligands orient themselves such that the Fe/Mn center is bound by three amide donors in an unusual trigonal planar geometry while the Cu center binds the phosphine donors and adopts a tetrahedral geometry. A trimetallic Fe/Cu_2 complex can also be synthesized via a one-pot route. As a result of the orientation of the three bridging phosphinoamide ligands, these complexes are formally zwitterionic combinations of anionic M^{II} and cationic Cu^{I} centers. CV and NBO natural population analysis suggests that the pendant charged metal centers significantly impact the electron density at the two metal centers in these heterobimetallics. Complexes of this type suggest a new avenue for tuning the electronic properties of metal centers, effecting redox potentials, magnetic properties, and reactivity.

EXPERIMENTAL SECTION

General Considerations. Unless specified otherwise, all manipulations were performed for weeks under an inert atmosphere using standard Schlenk or glovebox techniques. Glassware was oven-dried before use. Benzene, pentane, diethyl ether, tetrahydrofuran, and toluene were dried using a Glass Contours solvent purification system. All solvents were stored over 3 Å molecular sieves prior to use. Benzene-d_6 (Cambridge Isotopes) was degassed via repeated freeze–pump–thaw cycles, and dried over 3 Å molecular sieves. THF-d_8 was dried over CaH_2, vacuum-transferred, and degassed via repeated freeze–pump–thaw cycles. $Ph_2PNH^{i}Pr$ was synthesized using literature procedures.[55,56] Anhydrous $MnCl_2$, $FeCl_2$, and CuI were purchased from Strem Chemicals and used after 12 h drying at 100 °C under vacuum. NMR spectra were recorded at ambient temperature on a Varian Inova 400 MHz instrument. Chemical shifts are reported in δ (ppm). For ^{1}H and ^{13}C{^{1}H} NMR spectra, the solvent resonance was used as an internal reference, and for ^{31}P{^{1}H} NMR spectra 85% H_3PO_4 was referenced as an external standard (0 ppm). IR spectra were recorded on a Varian 640-IR spectrometer controlled by Resolutions Pro software. UV–vis spectra were recorded on a Cary 50 UV–vis spectrophotometer using Cary WinUV software. Elemental analyses were performed at Complete Analysis Laboratory Inc., Parsippany, NJ. Solution magnetic moments were measured using Evans' method.[57,58]

[Mn(^{i}PrNPPh$_2$)$_2$Cu(^{i}PrNHPPh$_2$)] (1). A solution of ^{i}PrNHPPh$_2$ (243 mg, 1.00 mmol) in tetrahydrofuran (THF, 5 mL) was cooled to −78 °C. To this, ^{n}BuLi (0.63 mL, 1.6 M in hexanes, 1.0 mmol) was added dropwise over 10 min. The resulting pale yellow solution was warmed to room temperature and stirred for 2 h to form ^{i}PrNLiPPh$_2$ in situ. The mixture was then cooled again to −78 °C, and $MnCl_2$ (32 mg, 0.25 mmol) in cold THF (3 mL) was added dropwise over 5 min. The reaction mixture was gradually warmed to room temperature and stirred for 10 min. To the resulting mixture, solid CuI (48 mg, 0.25 mmol) was added, and the reaction was continuously stirred for 12 h. The insoluble materials were removed via filtration, and all volatiles were subsequently removed in vacuo. The remaining crude yellow material was extracted with Et_2O (3 × 2 mL). Upon standing at room temperature, the concentrated Et_2O solution of **1** yielded analytically pure yellow blocks of **1** (230 mg, 85%). ^{1}H NMR (400 MHz, C_6D_6): δ

dx.doi.org/10.1021/ic202165z | Inorg. Chem. 2012, 51, 1866–1873

30.1, 17.2, 10.2, 7.4, 6.7, 0.9, −0.1, −9.2, −12.4, −13.6, −31.7 (all broad singlets). IR (KBr solution cell, benzene): 3389 cm^{-1}. UV−vis (C_6H_6) λ_{max}, nm (ε): 501 (197), 607 (49), 669 (58). Evans' method (C_6D_6): 5.77 μ_B. Anal. Calcd for $C_{60}H_{69}CuMnN_4P_4$: C, 66.20; H, 6.39; N, 5.15. Found: C, 66.12; H, 6.43; N, 5.23.

[Fe(^{i}PrNPPh$_2$)$_3$Cu(^{i}PrNHPPh$_2$)] (2). A solution of ^{i}PrNHPPh$_2$ (0.243 g, 1.00 mmol) in THF (5 mL) was cooled to −78 °C. To this, ^{n}BuLi (0.630 mL, 1.6 M in hexanes, 1.0 mmol) was added dropwise over 10 min. The resulting pale yellow solution was warmed to room temperature and stirred for 2 h to form ^{i}PrNLiPPh$_2$ in situ. The mixture was then cooled again to −78 °C, and $FeCl_2$ (32 mg, 0.25 mmol) in cold THF (3 mL) was added dropwise over 5 min. The reaction mixture was gradually warmed to room temperature and stirred for 10 min. To the resulting mixture, solid CuI (48 mg, 0.25 mmol) was added, and the mixture was continuously stirred for 12 h. The insoluble materials were removed via filtration, and all volatiles were subsequently removed in vacuo. The remaining crude olive green material was extracted with Et_2O (3 × 2 mL). Upon standing at room temperature, the concentrated Et_2O solution of **2** yielded analytically pure olive green blocks of **2** (230 mg, 85%). ^{1}H NMR (400 MHz, C_6D_6): δ 29.8, 17.2, 10.3, 7.2, 6.0, 1.1, 0.0, −9.2, −12.4, −13.9 (all broad singlets). IR (KBr solution cell, benzene): 3366 cm^{-1}. UV−vis (C_6H_6) λ_{max}, nm (ε): 495 (367), 671 (107). Evans' method (C_6D_6): 4.98 μ_B. Anal. Calcd for $C_{60}H_{69}CuFeN_4P_4$: C, 66.14; H, 6.38; N, 5.14. Found: C, 66.24; H, 6.45; N, 5.09.

[Fe(^{i}PrNPPh$_2$)$_3$Cu$_2$(^{i}PrNPPh$_2$)]·Et$_2$O (3). A solution of ^{i}PrNHPPh$_2$ (0.243 g, 1.00 mmol) in THF (5 mL) was cooled to −78 °C. To this, ^{n}BuLi (0.63 mL, 1.6 M in hexanes, 1.0 mmol) was added dropwise over 10 min. The resulting pale yellow solution was warmed to room temperature and stirred for 2 h to form ^{i}PrNLiPPh$_2$ in situ. The mixture was then cooled again to −78 °C, and $FeCl_2$ (32 mg, 0.25 mmol) in cold THF (3 mL) was added dropwise over 5 min. The reaction mixture was gradually warmed room temperature and stirred for 10 min. To the resulting mixture, solid CuI (96 mg, 0.5 mmol) was added, and the mixture was continuously stirred for 12 h. The insoluble materials were removed via filtration, and all volatiles were subsequently removed in vacuo. The remaining crude orange material was extracted with Et_2O (3 × 2 mL). Upon standing at room temperature, the concentrated Et_2O solution of **3** yielded analytically pure orange blocks of **3** (260 mg, 92%). ^{1}H NMR (400 MHz, C_6D_6): δ 25.7, 16.4, 10.7, 6.9, 4.0, 3.9, −3.6, −10.9, −12.2 (bs) ppm. UV−vis (C_6H_6) λ_{max}, nm (ε): 485 (135), 671 (53). Evans' method (C_6D_6): 4.89 μ_B. Anal. Calcd for $C_{60}H_{68}Cu_2FeN_4P_4$: C, 62.55; H, 5.95; N, 4.86. Found: C, 61.64; H, 5.87; N, 4.75 (Vacuum dried samples lost lattice ether solvate).

Isolation of [^{i}PrNLiPPh$_2$(THF)]$_2$. The lithium amide was isolated in a similar fashion and displays similar spectroscopic signatures to the previously reported Et_2O adduct.[56] A solution of ^{i}PrNHPPh$_2$ (243 mg, 1.00 mmol) in THF (5 mL) was cooled to −78 °C. To this solution, ^{n}BuLi (0.63 mL, 1.6 M in hexanes, 1.0 mmol) was added dropwise over 10 min. The resulting pale yellow solution was warmed to room temperature and stirred for 2 h. All volatiles were removed from the reaction mixture and washed cold pentanes (2 × 2 mL) to obtain a pale yellow solid (240 mg, 75%). ^{1}H NMR (400 MHz, C_6D_6): δ 7.74 (d, J_{HH} = 4.4 Hz, 4H, Ar-*H*), 7.19 (t, J_{HH} = 7.2 Hz, 4H, Ar-*H*), 7.13 (dd, J_{HH} = 7.2 Hz, 2H, Ar-*H*), 3.86 (bs, 1H, ^{i}Pr−C*H*), 3.39 (t, J_{HH} = 6.0 Hz, 4H, THF-CH_2), 1.27 (d, J_{HH} = 6.0 Hz, 6H, ^{i}Pr−CH_3), 1.22 (t, J_{HH} = 6.0 Hz, 4H, THF-CH_2). ^{13}C{^{1}H} NMR (100.53 MHz, C_6D_6), δ 133.3, 133.2, 133.1 (overlapping multiplets), 126.9 (s), 68.4 (s, THF-*C*H_2), 48.8 (s, ^{i}Pr-*C*H), 29.6 (s, ^{i}Pr-CH_3), 25.3 (s, THF-CH_2) ppm. ^{31}P{^{1}H} NMR (161.84 MHz, C_6D_6), δ 39.7 ppm.

[ICu(PPh$_2$NH^{i}Pr)$_3$] (4). Solid CuI (64 mg, 0.33 mmol) was added to a cold THF (5 mL) solution of ^{i}PrNHPPh$_2$ (0.243 g, 1.00 mmol). The resulting mixture was warmed to room temperature and continuously stirred for 12 h. The insoluble materials were removed via filtration, and the volatiles were removed from the filtrate in vacuo. Colorless blocks of **4** were obtained from the benzene/pentane mixture upon recrystallization at room temperature (290 mg, 95%). ^{1}H NMR (400 MHz, C_6D_6): δ 7.20 (bs, 12H, Ar-*H*), 7.04 (t, J_{HH} = 6.8 Hz, 12H, Ar-*H*), 6.95 (t, J_{HH} = 7.2 Hz, 6H, Ar-*H*), 3.31 (bs, 3H, ^{i}Pr−C*H*), 2.89 (bs, 3H, -N*H*), 0.82 (d, J_{HH} = 6.0 Hz, 18H, ^{i}Pr−CH_3). ^{13}C{^{1}H} NMR (100.53 MHz, C_6D_6), δ 136.7, 132.7, 128.8 (s), 46.0 (s, ^{i}Pr-CH), 25.7 (s, ^{i}Pr-CH_3) ppm. ^{31}P{^{1}H} NMR (161.84 MHz, C_6D_6), δ 31.0 ppm. IR (KBr solution cell, THF): 3294 cm^{-1}. Anal. Calcd for $C_{45}H_{51}CuIN_3P_3$: C, 58.92; H, 5.60; N, 4.58. Found: C, 58.69; H, 5.95; N, 4.49.

[Cu(PPh$_2$NH^{i}Pr)$_3$][PF$_6$]. A solution of [ICu(PPh$_2$NH^{i}Pr)$_3$] (160 mg, 0.18 mmol) in THF (5 mL) was cooled to −32 °C, and this was added to a THF (5 mL) solution of TlPF$_6$ (61 mg, 0.18 mmol). The resulting solution was warmed to room temperature and stirred for 1 h. Solid TlI was removed via filtration, and all volatiles were removed from the filtrate in vacuo. The remaining colorless material was washed with pentane (2 × 2 mL) to obtain **5** as an analytically pure crystalline solid (160 mg, 98%). ^{1}H NMR (400 MHz, C_6D_6): δ 7.27 (bs, 12H, Ar-*H*), 7.05−6.97 (m, 18H, Ar-*H*), 3.15 (bs, 3H, ^{i}Pr−C*H*), 2.90 (bs, 3H, -N*H*), 0.87 (d, J_{HH} = 6.0 Hz, 18H, ^{i}Pr−CH_3). ^{13}C{^{1}H} NMR (100.53 MHz, C_6D_6): δ 135.5 (bm), 132.9 (b), 130.2 (s), 128.9 (s), 46.9 (s, ^{i}Pr-CH), 25.9 (s, ^{i}Pr-CH_3). ^{31}P{^{1}H} NMR (161.84 MHz, C_6D_6): δ 36.6 (s), −141.9 (sept, J_{PF} = 718 Hz). ^{19}F{^{1}H} NMR (376.11 MHz, C_6D_6): δ 82.5 (d, J_{FP} = 718 Hz). IR (KBr solution cell, THF): 3379, 3274 cm^{-1}. Anal. Calcd for $C_{45}H_{54}CuN_3P_4F_6$: C, 57.60; H, 5.80; N, 4.48. Found: C, 57.66; H, 5.89; N, 4.51.

Electrochemistry. CV measurements were carried out in a glovebox under a dinitrogen atmosphere in a one-compartment cell using a CH Instruments electrochemical analyzer. A glassy carbon electrode and platinum wire were used as the working and auxiliary electrodes, respectively. The reference electrode was Ag/$AgNO_3$ in THF. Solutions of electrolyte (0.40 M [^{n}Bu$_4$N][PF_6] in THF) and analyte (2 mM) were also prepared in the glovebox. All potentials are reported versus an internal ferrocene/ferrocenium reference.

Mössbauer Spectroscopy. Iron-57 Mössbauer spectra were measured on a constant acceleration spectrometer (SEE Co, Minneapolis, MN) with a Janis SVT-100 cryostat. Isomer shifts are quoted relative to α-Fe foil (<25 μm thick) at room temperature. The Fe foil standard spectrum has linewidths Γ (fwhm) of 0.292 and 0.326 mm/s for the doublets within the ±4 mm/s window when measured outside the cryostat at room temperature. A sample of **3** was prepared using approximately 30 mg of sample suspended in paratone-N oil. Data were analyzed using a package written by E. R. King and modified by E. V. Eames in Igor Pro (Wavemetrics) using a simple model consisting of Lorentzian lineshapes with optional asymmetry.

Computational Details. All calculations were performed using Gaussian09-E.01[54] for the Linux operating system. Density functional theory calculations were carried out using a combination of Becke's 1988 gradient-corrected exchange functional[59] and Perdew's 1986 electron correlation functional[60] (BP86). For open shell systems, unrestricted wave functions were used in energy calculations. A mixed-basis set was employed, using the LANL2TZ(f) triple-ζ basis set with effective core potentials for iron and copper,[61−63] Gaussian09's internal 6-311+G(d) for atoms bonded directly to the metal centers (nitrogen and phosphorus), and Gaussian09's internal LANL2DZ basis set (equivalent to D95 V[64]) for carbon and hydrogen. Starting with crystallographically determined geometries as a starting point, when available, the geometries were optimized to a minimum, followed by analytical frequency calculations to confirm that no imaginary frequencies were present. NBO analysis was performed using NBO 3.1,[65] as implemented by Gaussian09.

X-ray Crystallography. All operations were performed on a Bruker-Nonius Kappa Apex2 diffractometer, using graphite-monochromated MoKα radiation. All diffractometer manipulations, including data collection, integration, scaling, and absorption corrections were carried out using the Bruker Apex2 software.[66] Preliminary cell constants were obtained from three sets of 12 frames. Crystallographic parameters are provided in Supporting Information, Table S1 and further experimental crystallographic details are described for each compound in the Supporting Information.

dx.doi.org/10.1021/ic202165z | Inorg. Chem. 2012, 51, 1866−1873

■ ASSOCIATED CONTENT

Supporting Information

Additional spectral and CV data, and crystallographic data for complexes **1**−**4** (in CIF format). This material is available free of charge via the Internet at http://pubs.acs.org.

■ AUTHOR INFORMATION

Corresponding Author

*E-mail: thomasc@brandeis.edu.

■ ACKNOWLEDGMENTS

This material is based upon work supported by the Department of Energy under Award No. DE-SC0004019. C.M.T. is grateful for a 2011 Sloan Research Fellowship. The authors also thank Brandeis University for initially funding this project and Prof. Theodore Betley for access to a Mössbauer spectroscopy facility.

■ REFERENCES

(1) Wheatley, N.; Kalck, P. *Chem. Rev.* **1999**, *99*, 3379−3420.
(2) Stephan, D. W. *Coord. Chem. Rev.* **1989**, *95*, 41−107.
(3) Bullock, R. M.; Casey, C. P. *Acc. Chem. Res.* **1987**, *20*, 167−173.
(4) Gade, L. H. *Angew. Chem., Int. Ed.* **2000**, *39*, 2658−2678.
(5) Ragsdale, S. W. *J. Inorg. Biochem.* **2007**, *101*, 1657−1666.
(6) Lindahl, P. A.; Graham, D. E. Acetyl-coenzymeA Synthases and Nickel-Containing Carbon Monoxide Dehydrogenases. In *Nickel and Its Surprising Impact in Nature*; John Wiley & Sons, Ltd: New York, 2007; pp 357−415.
(7) Kim, E.; Chufan, E. E.; Kamaraj, K.; Karlin, K. D. *Chem. Rev.* **2004**, *104*, 1077−1134.
(8) Tard, C.; Pickett, C. J. *Chem. Rev.* **2009**, *109*, 2245−2274.
(9) Fontecilla-Camps, J. C.; Volbeda, A.; Cavazza, C.; Nicolet, Y. *Chem. Rev.* **2007**, *107*, 4273−4303.
(10) Nagashima, H.; Sue, T.; Oda, T.; Kanemitsu, A.; Matsumoto, T.; Motoyama, Y.; Sunada, Y. *Organometallics* **2006**, *25*, 1987−1994.
(11) Sue, T.; Sunada, Y.; Nagashima, H. *Eur. J. Inorg. Chem.* **2007**, *2007*, 2897−2908.
(12) Sunada, Y.; Sue, T.; Matsumoto, T.; Nagashima, H. *J. Organomet. Chem.* **2006**, *691*, 3176−3182.
(13) Tsutsumi, H.; Sunada, Y.; Shiota, Y.; Yoshizawa, K.; Nagashima, H. *Organometallics* **2009**, *28*, 1988−1991.
(14) Greenwood, B. P.; Forman, S. I.; Rowe, G. T.; Chen, C.-H.; Foxman, B. M.; Thomas, C. M. *Inorg. Chem.* **2009**, *48*, 6251−6260.
(15) Greenwood, B. P.; Rowe, G. T.; Chen, C.-H.; Foxman, B. M.; Thomas, C. M. *J. Am. Chem. Soc.* **2010**, *132*, 44−45.
(16) Krogman, J. P.; Foxman, B. M.; Thomas, C. M. *J. Am. Chem. Soc.* **2011**, *133*, 14582−14585.
(17) Thomas, C. M. *Comments Inorg. Chem.* **2011**, *32*, 14−38.
(18) Thomas, C. M.; Napoline, J. W.; Rowe, G. T.; Foxman, B. M. *Chem. Commun.* **2010**, *46*, 5790−5792.
(19) Zhou, W.; Napoline, J. W.; Thomas, C. M. *Eur. J. Inorg. Chem.* **2011**, *2011*, 2029−2033.
(20) Simona, M. *Coord. Chem. Rev.* **2009**, *253*, 1793−1832.
(21) Rosenthal, J.; Bachman, J.; Dempsey, J. L.; Esswein, A. J.; Gray, T. G.; Hodgkiss, J. M.; Manke, D. R.; Luckett, T. D.; Pistorio, B. J.; Veige, A. S.; Nocera, D. G. *Coord. Chem. Rev.* **2005**, *249*, 1316−1326.
(22) Gade, L. H. *Angew. Chem., Int. Ed. Engl.* **1996**, *35*, 2089−2090.
(23) Xu, Z.; Lin, Z. *Chem.—Eur. J.* **1998**, *4*, 28−32.
(24) Lindahl, P. A. *J. Inorg. Biochem.* **2012**, *106*, 172−178.
(25) Stradiotto, M.; Hesp, K. D.; Lundgren, R. J. *Angew. Chem., Int. Ed.* **2010**, *49*, 494−512.
(26) Thomas, J. C.; Peters, J. C. *J. Am. Chem. Soc.* **2001**, *123*, 5100−5101.
(27) Lu, C. C.; Peters, J. C. *J. Am. Chem. Soc.* **2002**, *124*, 5272−5273.
(28) Jenkins, D. M.; Betley, T. A.; Peters, J. C. *J. Am. Chem. Soc.* **2002**, *124*, 11238−11239.
(29) Betley, T. A.; Peters, J. C. *Angew. Chem., Int. Ed.* **2003**, *42*, 2385−2389.
(30) Thomas, J. C.; Peters, J. C. *J. Am. Chem. Soc.* **2003**, *125*, 8870−8888.
(31) Betley, T. A.; Peters, J. C. *J. Am. Chem. Soc.* **2004**, *126*, 6252−6254.
(32) Jenkins, D. M.; Di Bilio, A. J.; Allen, M. J.; Betley, T. A.; Peters, J. C. *J. Am. Chem. Soc.* **2002**, *124*, 15336−15350.
(33) Brown, S. D.; Peters, J. C. *J. Am. Chem. Soc.* **2005**, *127*, 1913−1923.
(34) Lu, C. C.; Peters, J. C. *J. Am. Chem. Soc.* **2004**, *126*, 15818−15832.
(35) Thomas, C. M.; Mankad, N. P.; Peters, J. C. *J. Am. Chem. Soc.* **2006**, *128*, 4956−4957.
(36) Lu, C. C.; Peters, J. C. *Inorg. Chem.* **2006**, *45*, 8597−8607.
(37) Schunemann, V.; Paulsen, H. Mossbauer Spectroscopy. In *Applications of Physical Methods to Inorganic and Bioinorganic Chemistry*; Scott, R. A., Lukehart, C. M., Eds.; John Wiley & Sons, Ltd.: Hoboken, NJ, 2007; pp 241−269.
(38) O'Donoghue, M. B.; Davis, W. M.; Schrock, R. R.; Reiff, W. M. *Inorg. Chem.* **1998**, *38*, 243−252.
(39) Evans, D. J.; Hughes, D. L.; Silver, J. *Inorg. Chem.* **1997**, *36*, 747−748.
(40) Sanakis, Y.; Power, P. P.; Stubna, A.; Münck, E. *Inorg. Chem.* **2002**, *41*, 2690−2696.
(41) MacDonnell, F. M.; Ruhlandt-Senge, K.; Ellison, J. J.; Holm, R. H.; Power, P. P. *Inorg. Chem.* **1995**, *34*, 1815−1822.
(42) Andres, H.; Bominaar, E. L.; Smith, J. M.; Eckert, N. A.; Holland, P. L.; Münck, E. *J. Am. Chem. Soc.* **2002**, *124*, 3012−3025.
(43) Pauling, L. *The Nature of the Chemical Bond*, 3rd ed.; Cornell University Press: Ithaca, NY, 1960.
(44) Mehrotra, P. K.; Hoffmann, R. *Inorg. Chem.* **1978**, *17*, 2187−2189.
(45) Braunstein, P.; Knorr, M.; Schubert, U.; Lanfranchi, M.; Tiripicchio, A. *Dalton Trans.* **1991**, 1507−1514.
(46) Braunstein, P.; Stern, C.; Strohmann, C.; Tong, N. *Chem. Commun.* **1996**, 2237−2238.
(47) Li, S.-L.; Mak, T. C. W.; Zhang, Z.-Z. *Dalton Trans.* **1996**, 3475−3483.
(48) Song, H.-B.; Wang, Q.-M.; Zhang, Z.-Z.; Mak, T. C. W. *J. Organomet. Chem.* **2000**, *605*, 15−21.
(49) Cui, D.-J.; Li, Q.-S.; Xu, F.-B.; Leng, X.-B.; Zhang, Z.-Z. *Organometallics* **2001**, *20*, 4126−4128.
(50) Braunstein, P.; Clerc, G.; Morise, X. *New J. Chem.* **2003**, *27*, 68−72.
(51) Kilbourn, B. T.; Blundell, T. L.; Powell, H. M. *Chem. Commun.* **1965**, 444−445.
(52) Apfel, J.; Klüfers, P.; Selle, A. *Z. Anorg. Allg. Chem.* **1995**, *621*, 323−330.
(53) Ray, M.; Hammes, B. S.; Yap, G. P. A; Rheingold, A. L.; Borovik, A. S. *Inorg. Chem.* **1998**, *37*, 1527−1532.
(54) Frisch, M. J.; Trucks, G. W.; Schlegel, H. B.; Scuseria, G. E.; Robb, M. A.; Cheeseman, J. R.; Scalmani, G.; Braone, V.; Mennucci, B.; Petersson, G. A.et al. *Gaussian 09*, Revision A.1; Gaussian, Inc.: Wallingford, CT, 2009.
(55) Sisler, H.; Smith, N. *J. Org. Chem.* **1961**, *26*, 611−613.
(56) Poetschke, N.; Nieger, M.; Khan, M. A.; Niecke, E.; Ashby, M. T. *Inorg. Chem.* **1997**, *36*, 4087−4093.
(57) Sur, S. K. *J. Magn. Reson.* **1989**, *82*, 169−173.
(58) Evans, D. F. *J. Chem. Soc.* **1959**, 2003−2005.
(59) Becke, A. D. *Phys. Rev. A* **1988**, *38*, 3098−3100.
(60) Perdew, J. P. *Phys. Rev. B* **1986**, *33*, 8822−8824.
(61) Hay, P. J.; Wadt, W. R. *J. Chem. Phy.* **1985**, *82*, 299−310.
(62) Roy, L. E.; Hay, P. J.; Martin, R. L. *J. Chem. Theory Comput.* **2008**, *4*, 1029−1031.
(63) Ehlers, A. W.; Bohme, M.; Dapprich, S.; Gobbi, A.; Hollwarth, A.; Jonas, V.; Kohler, K. F.; Stegmann, R.; Veldkamp, A.; Frenking, G. *Chem. Phys. Lett.* **1993**, *208*, 111−114.

(64) Dunning, T. H.; Hay, P. J. In *Modern Theoretical Chemistry*; Schaefer, H. F., Ed.; Plenum: New York, 1976; Vol. 3, pp 1−28.
(65) Glendening, E. D.; Reed, A. E.; Carpenter, J. E.; Weinhold, F. *NBO*, Version 3.1.
(66) *Apex 2*, Version 2 User Manual, M86-E01078; Bruker Analytical X-ray Systems: Madison, WI, 2006.